Cooperativity in Forced Unfolding of Tandem Spectrin Repeats

Richard Law,* Philippe Carl,* Sandy Harper,† Paul Dalhaimer,* David W. Speicher,*† and Dennis E. Discher*†
*Biophysical Engineering Lab, Institute for Medicine and Engineering; and School of Engineering and Applied Science, University of Pennsylvania, Philadelphia, Pennsylvania 19104-6315, and †Structural Biology Program, The Wistar Institute, Philadelphia, Pennsylvania 19104

ABSTRACT Force-driven conformational changes provide a broad basis for protein extensibility, and multidomain proteins broaden the possibilities further by allowing for a multiplicity of forcibly extended states. Red cell spectrin is prototypical in being an extensible, multidomain protein widely recognized for its contribution to erythrocyte flexibility. Atomic force microscopy has already shown that single repeats of various spectrin family proteins can be forced to unfold reversibly under extension. Recent structural data indicates, however, that the linker between triple-helical spectrin repeats is often a contiguous helix, thus raising questions as to what the linker contributes and what defines a domain mechanically. We have examined the extensible unfolding of red cell spectrins as monomeric constructs of just two, three, or four repeats from the actin-binding ends of both α- and β-chains, i.e., α_{18-21} and β_{1-4} or their subfragments. In addition to single repeat unfolding evident in sawtooth patterns peaked at relatively low forces ($<$50 pN at 1 nm/ms extension rates), tandem repeat unfolding is also demonstrated in ensemble-scale analyses of thousands of atomic force microscopy contacts. Evidence for extending two chains and loops is provided by force versus length scatterplots which also indicate that tandem repeat unfolding occurs at a significant frequency relative to single repeat unfolding. Cooperativity in forced unfolding of spectrin is also clearly demonstrated by a common force scale for the unfolding of both single and tandem repeats.

INTRODUCTION

For many cytoskeletal and adhesion proteins, length and extensibility are central to function, and most such proteins have repeating, multidomain structures that reflect this (Kreis and Vale, 1999). The list of such proteins is long and ranges notably from immunoglobulin (Ig) domain superfamily proteins which are β-sheet structures, including Ig cell adhesion molecules and titin, to spectrin repeat superfamily proteins such as actinin, fodrin, and spectrin which are α-helix structures. For all, the definition of a domain as an independently folded sub chain within a protein seems to apply, and recent single molecule studies on the mentioned proteins—primarily using atomic force microscopy (AFM) methods (Rief et al., 1997)—reinforce this by showing that many such domains can be forced to unfold in a stochastic, one-domain-at-a-time fashion. When compared to a growing list of forcibly unfolded protein domains, the triple-helical repeats of spectrins stand out as among the most facile of folds (Rief et al., 1999; Lenne et al., 2000). Perhaps unique in another respect, available tandem repeat crystal structures for both chicken brain αII-spectrin (Grum et al., 1999) and the full four-repeat rod domain of α-actinin (Ylanne et al., 2001) show contiguous helices rather than flexible linkers between adjacent domains (Fig. 1).

The red cell, with its αI,βI-spectrin network of cross-linked actin protofilaments, is well-known for its resilient elasticity (Mohandas and Evans, 1994) but the submolecular basis for network softness is not completely clear. Disordered rather than helical linkers in spectrin seem reasonable, and electron microscopy has certainly indicated that different tissue forms of spectrin possess different stiffnesses or persistence lengths (Coleman et al., 1989). However, the high homology between α-actinin's four repeat rod domain and at least the four repeat, actin-binding ends of red cell αI- or βI-spectrins leads us to expect contiguous helices between these tandem erythroid repeats. Helical linkers are intriguing in their implications for spectrin extensibility and red cell elasticity, because domain unfolding might explain both thermal-softening (Waugh and Evans, 1979) and strain-softening of the intact erythrocyte network (Markle et al., 1983; Lee and Discher, 2001). Moreover, recent solution denaturation studies on purified, recombinant spectrin demonstrate that tandem repeats unfold in concert as a single unit, just as single domains do (MacDonald and Pozharski, 2001). Although tensile stresses directed from the N to C terminus of a protein chain could prove very different, in principle (Paci and Karplus, 2000), such directed forces are certainly more relevant to spectrin's physiological function. For multistate unfolding processes—such as tandem versus single repeat unfolding—requisite forces as well as relative probabilities can be measured by AFM methods if sufficiently large ensembles are thoroughly enumerated.

AFM studies of full-length red cell spectrin by Rief et al. (1999) show (one) extra-long unfolding event near the beginning of one illustrated sawtooth pattern; Rief et al. suggested this to be a tandem repeat unfolding event. To further elaborate such pathways of spectrin repeat unfolding, we have applied the AFM method of single molecule mechanics to purified two, three-, and four-repeat constructs (Fig. 1) of red cell αI- or βI-spectrin monomers. Unfolding of the two domain constructs proves both revealing and

Submitted June 3, 2002, and accepted for publication September 4, 2002.
Address reprint requests to Dennis E. Discher, Biophysical Engineering Lab, 112 Towne Building, University of Pennsylvania, Philadelphia, PA 19104-6315. Tel.: 215-898-4809; Fax: 215-573-6334; E-mail: discher@seas.upenn.edu.

0006-3495/03/01/533/12 $2.00

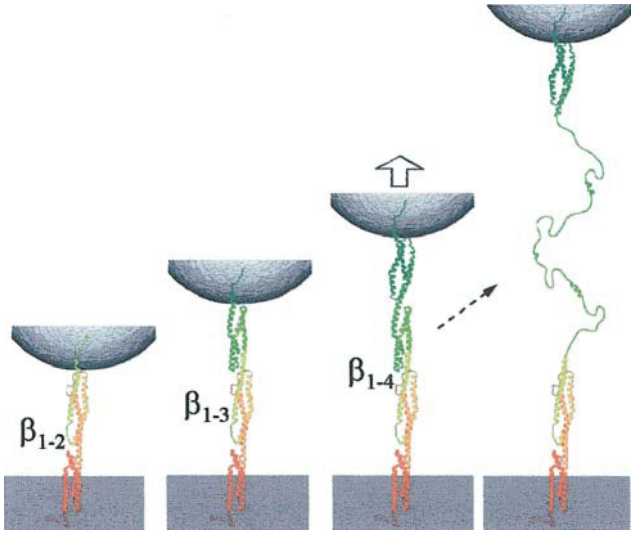

FIGURE 1 Forced extension and unfolding of 2, 3, or 4 repeat spectrin constructs by AFM. A single chain is shown adsorbed to both an AFM tip and a rigid substrate. Folded ribbon structures are those of α-actinin's rod domain (Ylanne et al., 2001). As a folded chain is tensed and a domain unfolds, the applied force relaxes and the chain extends, producing one sawtooth in a pattern of force relaxation. The far right shows one such repeat mostly unfolded and sketched as suggested by Brownian dynamics simulations of Paci and Karplus (2000).

unmistakable: the characteristic AFM–sawtooth patterns of unfolding appear similar to those for four domain constructs. Full analyses of the thousands of force spectrograms for each protein are done by first categorizing each according to the number of peaks as well as the sawtooth patterns' peak-to-peak lengths and force amplitudes. The categorization and analyses help rule out significant partial unfolding for these particular red cell spectrin constructs, whereas clear evidence for tandem repeat unfolding emerges in the carefully categorized length histograms. Finally, by introducing scatterplots of force versus length, a common force scale for unfolding both single and tandem repeats is clarified, identifying a cooperative mechanism of forced unfolding with serially adjacent spectrin repeats.

MATERIALS AND METHODS

Protein preparation

The four N-terminal repeats of the 17 domain erythroid βI-spectrin (β_{1-4}) and the last four repeats of αI-spectrin (α_{18-21}) (Table 1) were expressed recombinantly and prepared as described (Ursitti et al., 1996). Two and three repeat truncations of these two constructs were also studied. Protein was purified (and appeared as monomer; Ursitti et al., 1996) by gel permeation chromatography in phosphate-buffered saline (PBS) and kept on ice for AFM studies. Purified α- or β-spectrin constructs exist only as monomers in solution. Immediately before use, any protein aggregates were removed by centrifugation at 166,000g at 2°C for 1 h; dynamic light scattering was used to verify monodispersity prior to experiments.

An AFM experiment began by adsorbing 0.03–0.1 mg/ml protein (50 μL drop) for 15 min at room temperature onto either freshly cleaved mica or amino-silanized glass coverslips. The surface was then lightly rinsed with PBS and placed without drying, under the head of the AFM; all measurements were carried out in PBS. Lower protein concentrations generated minimal AFM results; higher protein concentrations showed higher unfolding forces, proving consistent with the conclusions below which indicate that domains in multiple, parallel chains will be forced to unfold all at once. Fluorescence imaging of labeled spectrin demonstrated homogeneous adsorption to the surface, and AFM imaging after scratching the surface further showed that no more than a monolayer of molecules covered the substrate (Carl et al., 2001).

TABLE 1 Primary structure properties of spectrin constructs (*aa*, amino acid). Domain and total contour lengths, l_c and L_c respectively, have been calculated with a peptide length of 0.37 nm

Domain	Number of aa	Contour, l_c (nm)	Domain	Number of aa	Contour, l_c (nm)
α21	111	41.0	β1	120	44.3
α20	114	42.1	β2	114	42.1
α19	107	39.5	β3	109	40.2
α18	109	40.2	β4	106	39.1
extra	9	3.3	*extra*	2	0.7
Total, L_c		166.1			166.4
Average		41.5			41.6

Dynamic force spectroscopy

Two AFMs were used with similar results: *1)* a Nanoscope IIIa Multimode AFM (Digital Instruments, Santa Barbara, CA) equipped with a liquid cell and *2)* an Epi-Force Probe from Asylum Research. Sharpened silicon nitride (SiN_3) cantilevers (Park Scientific, Sunnyvale, CA) of nominal spring constant $k_C = 10$ pN/nm were commonly used, with equivalent results obtained using 30-pN/nm cantilevers. k_C was measured for each cantilever by instrument-supplied methods, and additional calibrations were performed as described previously (Carl et al., 2001). Experiments (at ~23°C) were typically done at imposed displacement rates of 1 nm/ms as well as at 0.5 and 5 nm/ms. For any one speed, thousands (e.g., 6000–7000) of surface-to-tip contacts were generally collected and later analyzed with the aid of a custom, semiautomated, visual analysis program. For a many-hour experiment, initial results compared very favorably with results obtained near the end of the experiment. Nearly all of the data was thus analyzed without discarding much data as done in earlier studies of monomeric spectrin (Rief et al., 1999; Lenne et al., 2000).

RESULTS AND DISCUSSION

Sawtooth patterns with extra-long intervals

AFM-imposed extension of either the two, three, or even four domain constructs of spectrin all yield the widely recognized sawtooth patterns of forced unfolding (Fig. 2). The finding that both of the two domain constructs, α_{20-21} and β_{1-2}, can be extensibly unfolded by AFM appears to be particularly noteworthy. Unfolding of two domains is surprising in that a minimal amount of polypeptide is available for adsorption to both tip and substrate. Regardless of construct length, the force-extension spectrograms here reproduce several key features already found for a range of monomeric spectrin chains (Rief et al., 1999; Lenne et al., 2000). First, the heights of the force peaks are again found to be less than ~50 pN which is clearly much smaller than the

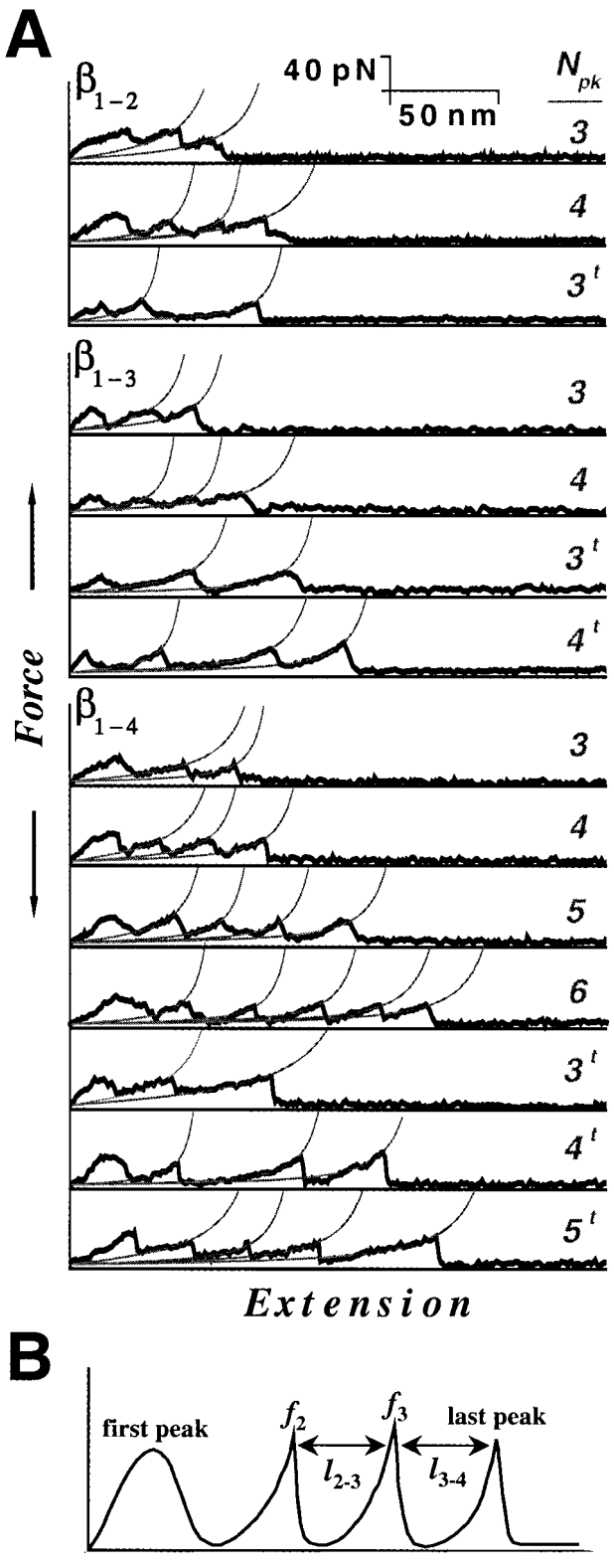

FIGURE 2 Force-extension spectrograms. (*A*) Force-extension curves for 2, 3, or 4, domain β-spectrin constructs. Peaks in the sawtooth patterns are characteristic of unfolding and show, consistent with random attachment, various numbers of peaks, N_{pk}. Some force spectrograms show extra-long unfolding intervals which reflect tandem repeat unfolding events. Force peaks after the first are less symmetric and are fit, for simplicity, by the WLC model $f(x) = (k_B T/p)\,[(x/L_C) + 0.25/(1 - x/L_C)^2 - 0.25]$ where x is chain extension and L_C is the contour length appropriate to the number of unfolded repeats. The fitted persistence length, p, that characterizes the minimal flexible length of an unfolded domain averaged 0.5 nm, consistent with prior reports (Rief et al., 1999) but shorter than what might be expected for a random coil polypeptide. This may therefore suggest a more structured state of unfolding (Paci and Karplus, 2000). Unless otherwise indicated, the imposed rate of extension for all of the results shown was 1 nm/ms. (*B*) Sketch of an $N_{pk} = 4$ spectrogram. The first peak and the height of the last peak are desorption events and ignored in the analyses. Peak forces and peak-to-peak lengths that are analyzed are indicated. The total unfolding length is the sum of all the indicated l_{i-j}.

150–300-pN forces reported for titin under similar rates of protein extension (0.01–10 nm/ms; see Rief et al., 1997). The force scale for spectrin unfolding appears independent of substrate effects inasmuch as similar forces had already been obtained with spectrin physisorbed to both gold and mica substrates; similar results are also found with amino-silanized glass (positively charged). Given the relatively low isoelectric points of these spectrin constructs (i.e., net negative charge; see Ursitti et al., 1996), the AFM results appear consistent with forced unfolding rather than forced desorption, although all experiments reported to date have used silicon-nitride AFM tips (with various k_C).

In addition to the heights of the force peaks, the exponentially increasing portions of the force-extension curves are reasonably well fit by a worm-like chain (WLC) model for entropic elasticity. As such, the force curves correspond to extension of an unfolded domain up to the point where another (still folded) domain in the chain unfolds. Evidence of partial unfolding in the first ~35 nm of extension (Lenne et al., 2000) has been given previously for two constructs of chicken brain α-spectrin: a flexibly concatenated 4-mer of repeat 16 and a native sequence 6-mer of repeats 13–18. Only the 4-mer showed a correlation between unfolding force and partial versus full unfolding. For the erythroid spectrins here, results below strongly suggest that partial unfolding is not a distinct occurrence. More apparent in the representative force-extension curves of Fig. 2 are a significant fraction of extensions which show extra-long length intervals between adjacent force peaks. Next to every spectrogram is an indication of the number of force peaks, N_{pk}; a superscript t demarks a spectrogram with an extra-long unfolding event which, based on criteria elaborated further below, will prove to be a tandem repeat unfolding event. Tandem events in the middle of force-extension spectrograms—rather than just between the last two peaks—are also important to note in the t-patterns.

Lastly, as elaborated later, the basic sawtooth patterns of unfolding, including the frequent observation of tandem repeat unfolding, are captured in Monte Carlo simulations of elastically coupled (Rief et al., 1997; Carl et al., 2001) multistate systems which kinetically compete. Simulations are a preferred method of modeling spectrin experiments compared to the WLC fits which require larger force peaks

and more nonlinear extensions to obtain reliable estimates of domain contour lengths.

Ensemble analyses of AFM extension

To assess the relative frequencies of states or pathways, it is critical that unbiased analyses be applied inasmuch as the typical AFM method of protein extension is intrinsically random in a number of ways. First, for a successful contact, an AFM tip comparable in radius to the size of an entire protein must come into contact with unseen molecule(s) preadsorbed to the substrate. The contact occurs, of course, at an unknown position or domain on the molecule. Second, in pulling the AFM tip away from the substrate, the molecule or molecules should bridge the gap between tip and substrate, but a long enough molecule could also form a loop that maintains two points of contact with either substrate or tip. Even at low protein concentrations, looped chains seem unavoidable for sufficiently long molecules. Third, inasmuch as a molecule is only physisorbed to the AFM tip (and the substrate also in the present studies), continued pulling will stress physisorbed attachment(s) and tend to disrupt them. Desorption could certainly occur before all possible domains between tip and substrate have been conformationally distended or unfolded. Marszalek et al. (2001) allude to some of these effects in pulling on polysaccharides that, like proteins, exhibit conformational transitions under force. With mixtures of polysaccharides, they point out that: ''On the average, one out of 10 trial contacts between the AFM tip and the substrate results in a force spectrogram that is unambiguously interpretable. In the other nine trials we picked up no molecules at all (the most common case) or we picked up too many molecules of similar length that produced a complicated, uninterpretable spectrogram.'' Polysaccharides tend to give less complicated, monotonically increasing spectrograms than multidomain proteins, so an analysis of more rather than less data can be a challenge. However, we show here that a thorough analysis can also provide important insights into both the existence and frequency of novel, less frequent states and pathways of protein unfolding. Arguably, unless one somehow knows ahead of time what force spectrogram is expected, any other selective sorting of single molecule data can introduce significant bias.

Number of peaks per sawtooth pattern, N_{pk}, versus the number of domains, D

Distributions of N_{pk} for the thousands of force-extension curves collected on any given construct provide a first characterization and categorization of all of the data in a given experiment (Fig. 3). They reveal Poisson-like distributions that highlight the stochastic nature of these types of AFM experiments. Percentage occurrences are explicitly indicated in each bar of the histograms of Fig. 3. Whereas contacts in PBS alone yield curves with $N_{pk} = 0$ or

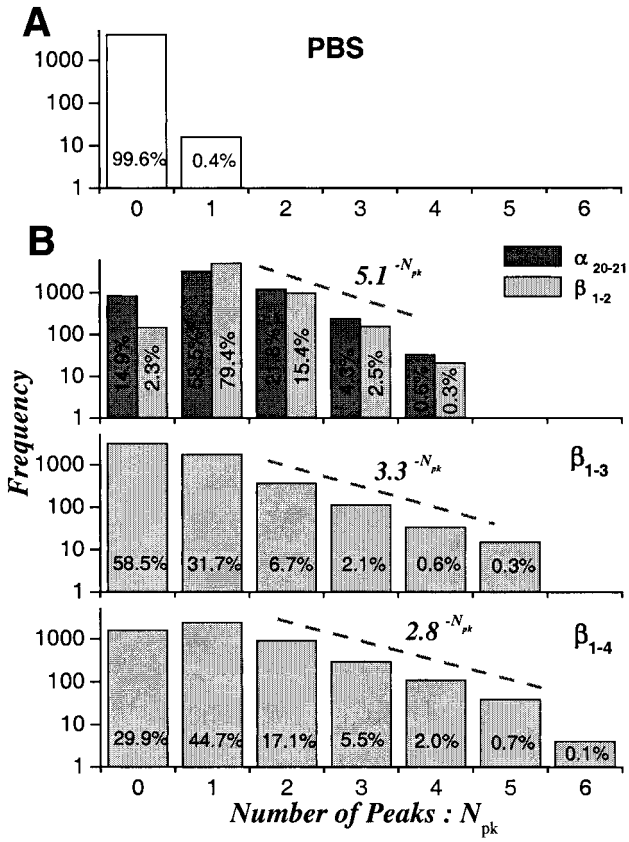

FIGURE 3 Number of peaks, N_{pk}, per extension in (A) buffer alone (PBS) without any protein, or (B) with preadsorbed spectrin constructs containing 2, 3, or 4 repeats. Each experiment involved 5000 contacts between AFM tip and substrate. For PBS alone, more than one peak was never seen. For spectrin, exponential decays of the form m^{-Npk} generally fit the multi-peak results between $1 < N_{pk} < max(N_{pk})$ with the indicated values for m.

1, the presence of protein is clearly associated with extension curves whenever $N_{pk} \geq 2$. As clarified below, however, curves with $N_{pk} = 2$ correspond to protein detachment from the surface (first peak) and then subsequent detachment from either the tip or surface (last peak), with no intervening unfolding events. Analyzable unfolding events require $N_{pk} \geq 3$, which are given as cumulated percentages in Table 2. At the low protein concentrations used, these events are seen to be a minor percentage ($<10\%$) of total contacts. Importantly, it has been established in the context of cell adhesion that for experiments to be predominantly in the single molecule limit the frequency of events should be 25% or less (e.g., Shao and Hochmuth, 1999). The percentages in Table 2 are well within this limit and thus appear consistent with the analyzable sawtooths being predominantly (though not exclusively) single molecule experiments.

The next goal was to correlate the N_{pk} distributions with the number of domains D in a given construct. Of minor importance, the recombinant spectrin chains used here do not contain chain-end cysteines which can certainly be useful for thio-gold attachments but which also potentiate end-linked

TABLE 2 Percentage of spectrograms with analyzable unfolding curves (i.e., $N_{pk} \geq 3$) out of 6000–7000 contacts

Construct	Spectrograms with $N_{pk} \geq 3$
α_{20-21}	4.9%
β_{1-2}	2.8%
β_{1-3}	3.0%
β_{1-4}	8.3%

dimers through disulfide bond formation. Such serial dimers would obviously introduce uncertainty into any correlation between N_{pk} and D. Thus, the two domain constructs of either α- or β-spectrin here are precisely that, and for these we find N_{pk} ranges from 0 to 4 after several thousand tip-to-surface contacts; buffer alone yields an occasional single peak, but never two peaks (Fig. 3 *A*). For a three domain β-construct, we find N_{pk} ranges from 0 to 5. For four domain constructs of either α- or β-spectrin, we find N_{pk} ranges from 0 to 6. Thus, for a given construct with D domains, the maximum number of peaks, $max(N_{pk})$, increases linearly with D (Fig. 4 *A*):

$$\mathrm{max}(\mathrm{N_{pk}}) = \mathrm{D} + \mathrm{b}; \mathrm{b} = 2 \qquad (1)$$

Importantly, because the slope of this correlation is unity, each added repeat yields exactly one added peak and no more than one added peak.

Partial unfolding would typically be expected to give two peaks per domain and a slope of 2 in Eq. 1, although other scenarios such as three peaks per two domains are also possible. Regardless, with exactly one peak per repeat, partial unfolding appears highly unlikely in the present experiments on red cell spectrin constructs.

An intercept of $b = 2$ in Eq. 1 accounts for: *1*) the last peak in any extension curve which no doubt corresponds to final desorption of the chain from either the AFM tip or the surface and *2*) the first peak in any extension curve which is most likely representative of initial desorption of the chain or tip rather than unfolding. As already indicated for buffer alone, the tip occasionally sticks to the substrate and gives a single peak. In addition, the first peak often stands out as the most symmetric peak in a spectrogram (see Fig. 2); this seems to be a general observation of others as well (Yang et al., 2000). Because of these general interpretations of the extension curves implied by Eq. 1, only spectrograms with $N_{pk} \geq 3$ were shown previously in Fig. 2 and thus analyzed in further depth below.

When fitted for $N_{pk} \geq 2$, the N_{pk} distributions consistently show a decay with N_{pk} which we fit to $\sim m^{-N_{pk}}$. The factor m provides a measure of the m-fold fewer ways of achieving one more unfolded domain (single and tandem) spanning the gap between tip and surface. The factor m undoubtedly reflects a random desorption process, but it also clearly shows a trend with D (Fig. 4 *B*): m decreases exponentially from ~5 to ~3 with D increasing from 2 to 4. Relevant desorption models will be reported elsewhere, but this

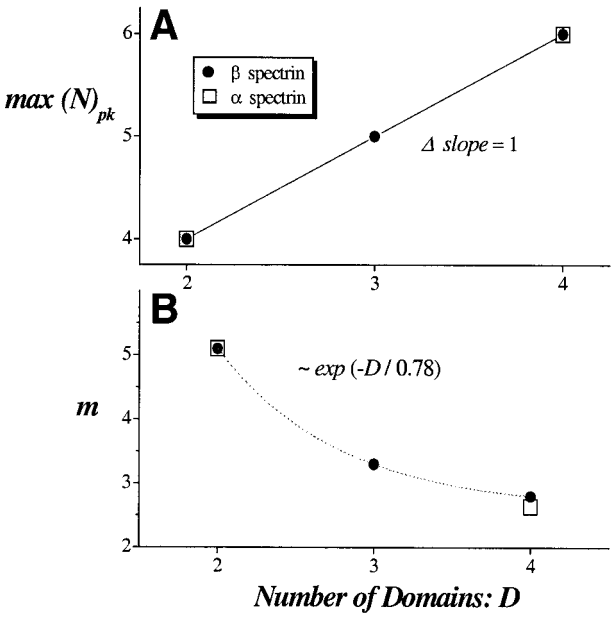

FIGURE 4 Dependence of N_{pk} histogram characteristics on the number of repeating domains, D. (*A*) Plot of $max(N_{pk})$ versus D shows a linear relationship of unit slope. (*B*) Plot of the factors m in the m^{-Npk} fits of Fig. 3 versus D. The decay is fit with a simple exponential and suggests a convergent process for unfolding an increasing number of repeats.

decrease in m with D provides a simple measure of the increased number of ways of unfolding domains when more domains, or degrees of freedom, are present. A simple calculation also suggests this: with $D = 2$, there are at most three unfolding pathways inasmuch as unfolding can involve one tandem repeat event or, in lieu of this, two single repeat events. With $D = 4$, in contrast, there are not only four possible single repeat events but also a combination of these with three tandem repeat events. The mutually exclusive nature of some of the single plus tandem repeat events combined with an unknown frequency of attachment to middle domains versus chain ends, and also loops versus single chains, makes the partitioning statistics for N_{pk} too complicated for further analysis here. Nonetheless, this empirical relation could prove useful in extrapolation to more physiological spectrins that have much larger D than those tested here.

Increased unfolding length as *D* increases

The total unfolding length, L_{unf}, for α- or β-spectrin constructs of two, three, or four domains (Fig. 5 shows β-spectrin) are found in cumulated histograms to be suitably bounded by single chain contour length limits that obviously increase with D (Table 1). The longer constructs show just two to three events (out of the hundreds analyzed) which exceed the theoretical contour lengths in Fig. 5 by ~25 nm or less; these few events probably reflect noise and baseline

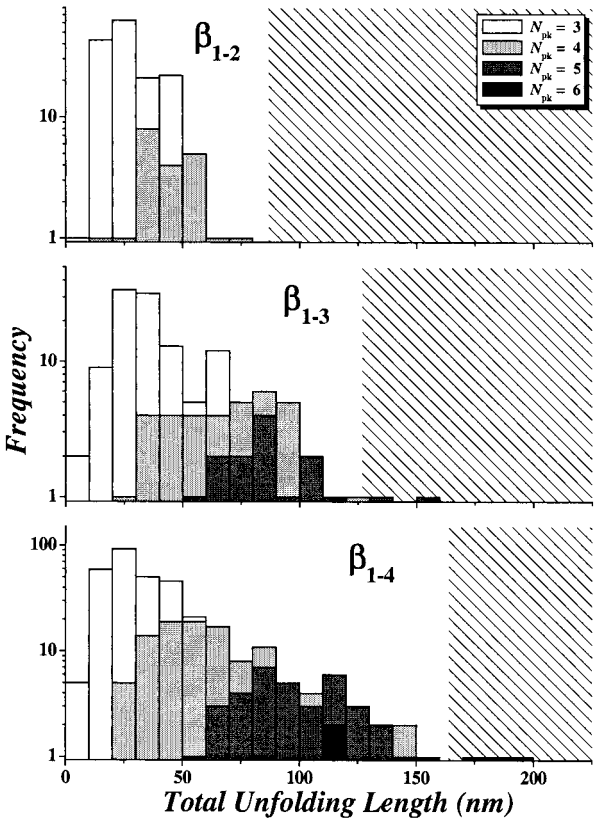

FIGURE 5 Distributions of total unfolding lengths, L_{unf}, obtained from the sawtooth-shaped extension curves beyond the first (nonspecific) peaks. The diagonally hatched regions correspond to fully stretched contour lengths, L_c (see Table 1), which define generic limits of extension.

drift with magnified effects in the longest extensions. The bound appears consistent with both monomeric chains and a lack of any higher order spectrin aggregates in solution (see Methods). Using the known ~25-nm end-to-end length of α-actinin's four-repeat rod domain (Ylanne et al., 2001), the unfolding lengths for the homologous four domain α- or β-spectrin constructs are readily calculated to be up to six- to sevenfold longer. It is also clear that L_{unf} increases with N_{pk} in an extension curve. Domain unfolding thus visibly modulates extensibility.

For titin constructs, Fernandez and co-workers (Marszalek et al., 1999) have already shown that the slope of $\langle L_{unf} \rangle$ versus N_{pk} can provide subnanometer estimations of domain unfolding length. However, because the thermal noise floor in the force measurements here is a significant $\sim(k_C\, k_B T)^{1/2} \approx 6$ pN, the much lower forces involved in unfolding spectrin repeats compared to titin repeats leads to much broader L_{unf} distributions for spectrin and therefore much greater uncertainty. An even more systematic problem here is that the combination of unfolding both single and tandem repeats will artificially reduce N_{pk} whereas fewer total peaks appear in a spectrin spectrogram when tandem repeats unfold.

Bimodal unfolding lengths-dependence on N_{pk}

Distributions of both the peak-to-peak unfolding lengths, l_{pk-pk}, and the heights of the force peaks (Figs. 6 and 7) provide the most succinct summaries of the thousands of force-extension sawtooth patterns that constitute an experiment. Compared to the present full analyses aimed at elucidating the various pathways of αI- and βI-spectrin unfolding, past experiments on different spectrins by both Rief et al. (1999) and Lenne et al. (2000) appear to have been more selective in analyses of force-extension spectrograms: curves containing, for example, 'high' force peaks were set aside (although precise selection criteria seem unclear). Nonetheless, published length and force distributions for spectrin generally appear broader than those for titin, consistent with spectrin's more facile unfolding processes. The length histograms here for spectrin are distinct from those for titin in another respect as well: for spectrin, they are bimodal.

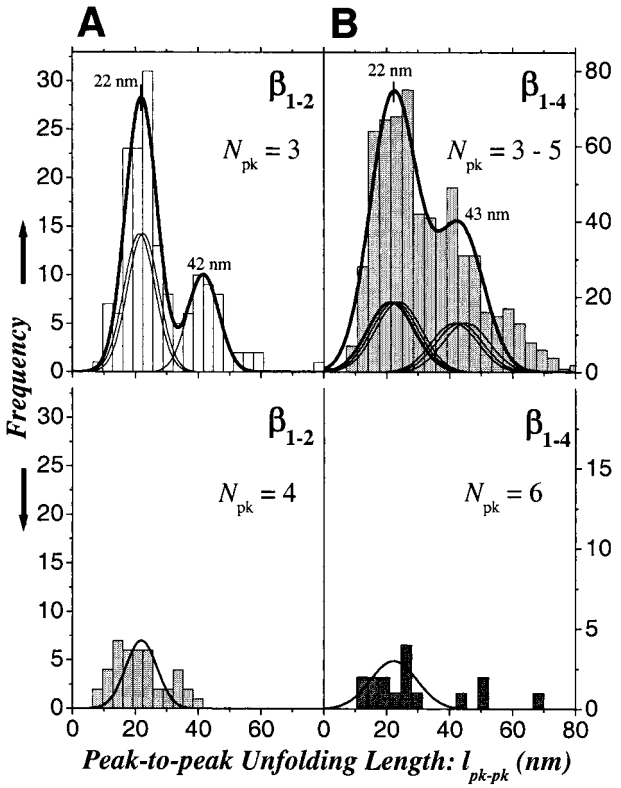

FIGURE 6 Histograms of peak-to-peak unfolding lengths for sawtooth extensions of (*A*) β_{1-2}-spectrin and (*B*) β_{1-4}-spectrin. The upper two bimodal histograms show results for $N_{pk} < max(N_{pk})$. The major peaks were fitted with sums of Gaussians that reflect proportional contour lengths for single repeats (see Table 1). The minor peaks were likewise fitted but with contour lengths of tandem repeats. The overall sum of all the Gaussians is indicated by the heavy black line; a factor of about two between the major and minor peaks is apparent. The lower two histograms show results only for $N_{pk} = max(N_{pk})$ and are found to be mostly enveloped by the major peaks, i.e., single repeat peaks, of the upper histograms.

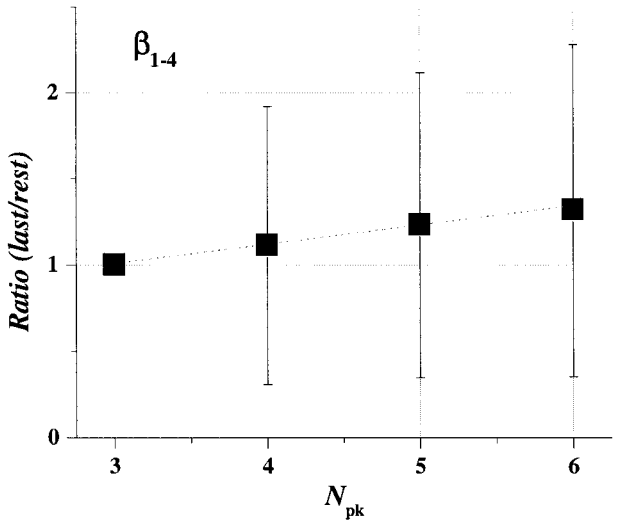

FIGURE 7 As a function of N_{pk} for β_{1-4}-spectrin, the plot shows the unfolding length of the last peak-to-peak interval divided by the average unfolding length of the previous intervals. The linear fit shows that the ratio tends to increase by ~10% with each additional peak in the spectrogram. This implies that slack in an unfolded chain is increasingly stretched out as more protein is extended and unfolded.

Fits of β-spectrins' N_{pk}-categorized histograms of l_{pk-pk} (Fig. 6) account for the domains' different contour lengths (see l_c in Table 1) through sums of multiple Gaussians using l_c-proportioned means (Carl et al., 2001). For example, with $D = 2$ (Fig. 6 *A*), single repeat unfolding was accounted for in $N_{pk} = 3$ spectrograms by summing two equal-height Gaussians with means constrained by the ratio l_{c1}/l_{c2}; tandem repeat unfolding was accounted for by simultaneous fitting of a third Gaussian. For $D = 2$ and $N_{pk} = 3$, the bimodal fit yields a major peak at 22 nm and a more minor peak at 42 nm. The minor peaks' averages in Fig. 6 (22 nm) are also in very close agreement with the *overall* average (24–26 nm) estimated from Lenne et al (2000) for a 4-mer of a single spectrin repeat flexibly linked in series. However, consistent with our lack of evidence here for partial unfolding in N_{pk}, we also lack any clear indication in our l_{pk-pk} histograms for the partial unfolding which Lenne et al. (2000) reported as a minor peak (25–30% of their data) centered at 15–16 nm. As noted by Lenne et al., however, such events nearly always occurred in the very initial 35 nm of chain extension, and in the experiments here on distinct repeats pulled off of distinct substrates, the initial desorption peak plus domain heterogeneity could well prove obscuring. Recalling Eq. 1 and its implications, we nonetheless conclude that the first major peak in our l_{pk-pk} histograms corresponds to the length gained in unfolding most of a single repeat. In addition, the 42-nm peak occurring at almost exactly twice (1.91 in Fig. 6 *A*) the first is clearly indicative of tandem repeat unfolding.

Categorization of unfolding patterns based on N_{pk} is further revealing: $N_{pk} = 4$ spectrograms for $D = 2$ appear more monomodal and never show any $l_{pk-pk} > 42$ nm. Indeed, the major peak centered at 22 nm for $N_{pk} = 3$ also envelopes the results for $N_{pk} = 4$. In light of the previous conclusions that $N_{pk} = 4$ spectrograms correspond to the unfolding of just two domains (recall the first and last peaks are desorption peaks), the length data here clearly implies that the two domains are both single repeats, consistent with expectations.

In assessing the relative frequency of tandem repeat unfolding versus single repeat unfolding, one should first compare spectrograms of similar, total unfolding length. In other words, for $D = 2$, the frequency of the $N_{pk} = 3$ tandem repeat 42-nm peak (one event per spectrogram) should be compared to the frequency of the $N_{pk} = 4$ single repeat 22-nm peak (two events per spectrogram) inasmuch as the latter spectrogram should have approximately the same total unfolding length (i.e., 2 × 22 nm compared to 1 × 42 nm). Such a comparison of frequencies for β_{1-2} shows that tandem unfolding (~35–45 events) occurs with almost equal probability to single repeat unfolding (~35–45 events). The range of uncertainty arises from the overlapping widths of the bimodal distributions. Similar results are found for α_{20-21}: ~80–90 tandem $N_{pk} = 3$ events versus ~70–80 single repeat $N_{pk} = 4$ events. Thus to a first approximation, analysis of the relative frequency of single repeat unfolding events versus tandem repeat unfolding events suggests an almost equal probability for the present constructs.

The ability to unfold two domain constructs with length-limited pathways of unfolding is clearly useful and revealing. Moreover, the bimodal means for $D = 2$ are in very good agreement with those for four domain constructs (Fig. 6 *B*): for $D = 4$ and $N_{pk} = 3$–5, the suitable bimodal fit yields a major peak at 22 nm and a more minor peak at 43 nm. Again, the factor of two (1.95) in bimodal means provides a clear indication of the major peak being single repeat unfolding and the minor peak being a signature for tandem repeat unfolding. In addition, the $N_{pk} = 6$ histogram shows that the majority (80%) of the l_{pk-pk} fall within the major envelope of single repeat unfolding events, consistent with $N_{pk} = 6$ corresponding to four single repeat events plus initial and final desorption events. The three events outside of the single repeat envelope evidently reflect overextension of the cumulated slack (Fig. 7) that develops toward the end of a long extension before final desorption terminates the spectrogram.

Lastly, subtracting an average folded domain size of ~6 nm (= 25 nm ÷ 4 domains) from the contour lengths of Table 1, the measured unfolding lengths of 22–24 nm are only about two-thirds of the adjusted mean contour lengths. This suggests that an unfolded domain is not fully stretched before the unfolding of the next domain occurs. Helical structures could certainly persist in unfolding (see Fig. 1) as indicated in Brownian dynamics simulations of Paci and Karplus (2000). Such a result is again consistent with both broader distributions and lower forces for unfolding spectrin in comparison, for example, to titin whose unfolding lengths

approach theoretical contour lengths at 5–10-fold higher forces. For spectrin, however, the freely-fitted factor of nearly 2.0 between the major and minor length peaks also provides a strong indication of two-thirds unfolding for a tandem pair of in-series repeats. It thus appears clear that Rief et al.'s brief mention of extra-long unfolding events (Rief et al., 1999) indeed corresponds to tandem repeat unfolding.

Bimodal distributions of unfolding forces

Revisiting the sawtooth patterns of Fig. 2, the heights of the force peaks that immediately precede the tandem unfolding intervals do not appear significantly higher than those required to unfold single repeats. In other words, the force to unfold a tandem repeat is the same as the force required to separately unfold a single repeat. Nonetheless, force distributions for unfolding spectrin (Fig. 8) appear bimodal with Gaussian means differing once again by ~2. Despite this, the scatterplots that follow, which pair a given unfolding length with the appropriate unfolding force (Fig. 9), clearly suggest that the factor of 2 reflects unfolding in one chain, two chains, or a loop in a chain, rather than unfolding tandem repeats versus single repeats.

Additional features are shared by the bimodal length and bimodal force histograms (Figs. 6 and 8, respectively). First, major peaks are clear and more prominent than right-shifted minor peaks; the major peak is also, once again, more prominent for $D = 2$ than for $D = 4$. Second, as with the length distributions, the bimodal force distributions for $D = 2$ and $D = 4$ exhibit nearly the same means; less clear or convincing in significance are slightly shorter lengths and smaller forces consistently found for $D = 2$ compared to $D = 4$ (for both α- and β-constructs).

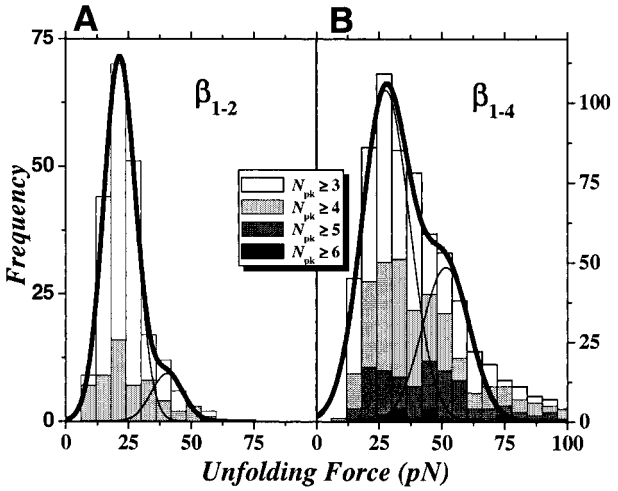

FIGURE 8 Histograms of unfolding forces for sawtooth extensions of (*A*) β_{1-2}-spectrin and (*B*) β_{1-4}-spectrin. The bimodal histograms were fitted with two Gaussians of the same width, and the overall sums of the Gaussians are indicated by heavy black lines.

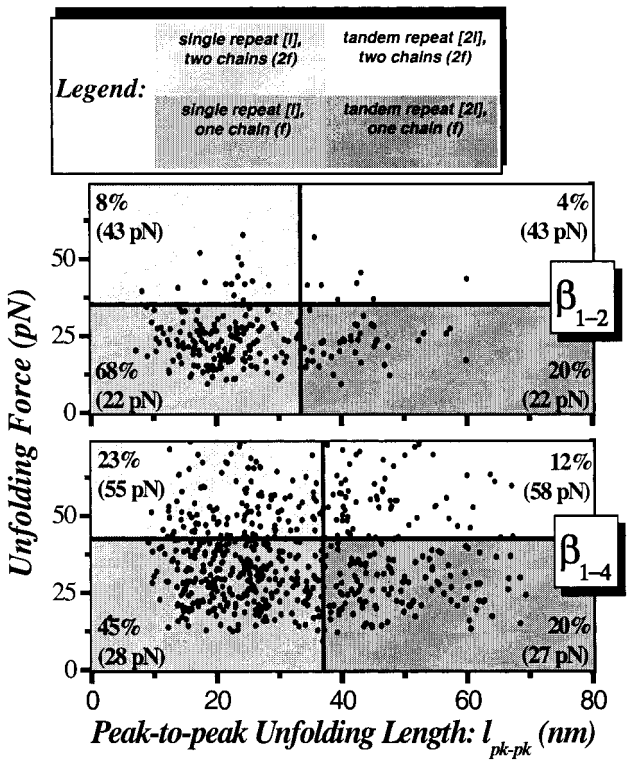

FIGURE 9 Scatterplots of unfolding force versus unfolding length. Dividing lines are obtained from the intersection between the major and minor Gaussians of Figs. 6 and 8 and thus represent a stringent if simplistic separation of unfolding processes or states. The legend at top represents the simplest interpretation of these states in terms of unit unfolding length, *l*, and unit unfolding force, *f*, of a single repeat. The lower two quadrants correspond to single chain unfolding, both single and tandem repeat unfolding, as indicated. The fraction of data points within each of the four quadrants is indicated as a percentage of total data points together with the quadrant-average force in parentheses.

Scatterplots of force-length pathways: tandem repeats

Scatterplots of unfolding force versus unfolding length shown in Fig. 9 prove most revealing of the multiple unfolding processes that underlie the experiments. Applying the bimodal divisions of Figs. 6 and 8 to the respective scatterplots is seen to divide each scatterplot into four quadrants or states. Most important, if tandem repeat unfolding were to require a force that is twofold higher than single repeat unfolding, then data points would concentrate in the lower left and upper right quadrants, i.e., along a diagonal in the scatterplot. Diagonalization is not observed. All four quadrants contain a significant number of data points, although data points are not evenly distributed between quadrants. The color code above Fig. 9 succinctly identifies the hypothesized transitions; and the relative probability of each is explicitly written as a percentage above the quadrant-average force.

As with the bimodal distributions for length (Fig. 6), the two left-most quadrants differ in average length from the two

right-most by a factor of two. This ratio again corresponds to the unfolding of single versus tandem repeats. Inasmuch as the lower two quadrants also contain most of the data points, it becomes clear that this figure first of all emphasizes the conclusion that the unfolding of a tandem repeat requires the same force as the unfolding of a single repeat. For $D = 4$ and both α- and β-monomers, the two lowest force quadrants—which correspond to single chains—have nearly the same average forces which are in the range of 26–28 pN.

Average unfolding forces of 32 pN and ~50 pN at comparable protein extension rates of ~1 nm/ms were respectively reported by Rief et al. (1999) and Lenne et al. (2000), although their analyses and distinct systems potentially complicate direct comparisons. Furthermore, analysis of a single sawtooth pattern for full-length red cell spectrin illustrated in Fig. 6 of Rief et al. (1999) yields measures for both unfolding force and length of 30 ± 5 pN and 34 ± 11 nm which also prove consistent with our data. Indeed, the latter length is in very good agreement with 33–35 nm for our overall average length of combined single and tandem unfolding in $D = 4$ constructs.

Scatterplots of force-length pathways: two chains and loops

Forces in the upper two quadrants of the scatterplots are also seen to be essentially 2.0-fold higher than the forces in the lower two quadrants. The upper two quadrants are therefore understood to involve pulling on either two separate chains or a loop of a single chain that spans the gap between tip and surface. Again, inasmuch as previous solution studies indicate monomeric chains and a lack of self-association (Ursitti et al., 1996), loops are also unlikely to be self-interacting, i.e., repeats in one 'leg' of the loop should respond independently of repeats in the other 'leg'. Keeping in mind that each data point in the scatterplots represents one perceived unfolding event, it is important to address whether unfolding within two parallel chains (including two legs of a loop) should indeed appear simultaneous or in close synchrony.

Consider two fully folded protein chains that bridge the gap between the AFM tip and the substrate. As the gap is increased, the AFM cantilever deflects as the two protein chains resist the extension. The net force applied to the two chains therefore increases. Regardless of whether the domains are in parallel register or not, the protein chains are mechanically equivalent to two equivalent springs in parallel so that the net force, f_{net}, partitions equally between the two protein chains. In other words, the forces in the two chains, designated chain A and chain B, will be $f_A = f_B = \frac{1}{2} f_{net}$. If f^* is the force required to unfold a domain in a single protein, then unfolding becomes increasingly likely for either chain only as $f_{net} \rightarrow 2f^*$. Domain unfolding is a stochastic process whose time constant decreases exponentially with force as $\tau(f) = \tau_o\, exp(-f \times const)$, where τ_o is the lifetime of a stable fold that ranges from $\sim 10^{2-6}$ sec (Rief et al., 1999). Therefore, as $f_{net} \rightarrow 2f^*$, one of the chains (designated chain A) will unfold first and within a time $\tau(f^*) \sim$ ms–μs. Furthermore, as known from sawtooth patterns for a single protein, f_A will then decrease. However, the force on chain B remains very high because the relaxation of the force exerted by the cantilever takes a finite time, τ_R (ms). This is due to the hydrodynamic resistance on the cantilever. Thus within a time of $\sim \tau_R/10$ of unfolding chain A, the force on chain B suddenly becomes $f_B = f_{net} \sim 2f^*$. This exceptionally large force is entirely exerted on chain B. As such, the force effect on unfolding chain B is effectively squared: $\tau(2f^*) = \tau_o\, [exp(-f^* \times const)]^2$. This greatly increases the probability of unfolding. More precisely, forced unfolding is found to occur on time scales comparable to τ_R or faster, i.e., $\tau_o exp(-f^* \times const) \sim$ ms–μs, so that the additional factor of $exp(-f^* \times const)$ provides a very strong impetus for the unfolding of chain B before the cantilever relaxes. The perceived force to unfold the domains in the two parallel chains A and B is thus $\sim 2f^*$. Experimental results to be published separately on α-, β-spectrin heterodimers associated in parallel registry also clearly indicate a force scale for unfolding that approaches 2.

Finally, although the surface mass concentrations of protein are uniformly low, data points in the upper quadrants of the scatterplots are sparse for $D = 2$ compared to $D = 4$. This implies fewer of either two chain or loop events for $D = 2$. Whereas spectrin is known to have a persistence length of at least several nanometers (e.g., Lee and Discher, 2001) and each triple-helical repeat is likely to be stiff, a two domain construct of length ~10–15 nm is clearly stiffer and less likely (due to bending energy) to form a loop compared to a four domain construct. Therefore, given the sparseness of the high force results for $D = 2$, these upper quadrant results in the scatterplot probably reflect the extension of two chains rather than loops. Consequently, many of the additional upper quadrant, high force results for $D = 4$ seem likely to result from loops rather than two separate chains. A further implication is that longer chains are expected to give more loop results. This argues in favor of studying short chains especially when the protein's domains unfold at low forces.

The relative probabilities of states indicated in Fig. 9 are also revealing. As expected from the low protein concentrations used in these studies, the number of times that two chains (or a loop of one chain) are pulled upon is small in comparison to a single chain. The lower frequency of tandem repeat unfolding, in either one chain or two, is also consistent with rudimentary statistical expectations. Given four domains to unfold, no more than two pairs can unfold per chain, and so a relative occurrence of ~2:1 single:tandem repeat unfolding is a reasonable first guess. The scatterplots suggest that this simple estimate applies. Nonetheless, in defining a free energy difference by taking the log_n of probability ratios and multiplying by $k_B T$, all such differences are calculated to be less than $\sim 1\ k_B T$. Inasmuch as accessible

transition states define the critical points of choice for a system to follow one pathway or another, the $<k_BT$ difference implies that both single and tandem repeat unfolding have very similar transition state energies.

Cooperativity and the near-common force scale

To reiterate, Fig. 9 shows that for all of the constructs, single repeat unfolding forces are nearly identical to tandem repeat unfolding forces, on average. This appears true even when comparing the results for loops and two chains between the upper two quadrants. Concluding that these forces are essentially the same must be tempered, however, by: (*i*) the likelihood of small unfolding force variations between structurally distinct repeats (see Table 1), (*ii*) the considerable experimental error arising with the use of soft cantilevers (e.g., Carl et al., 2001), and (*iii*) the noise intrinsic to single molecule measurements especially when unfolding forces are low, as here. Nevertheless, the near-common force scale suggests that forced unfolding occurs through a near-common transition state, consistent with the energetic conclusions above which were based on the relative probabilities of single and tandem states (or processes).

The notion that tandem repeat unfolding is a process which cooperatively follows single repeat unfolding—requiring little additional force or free energy cost—appears analogous to the cooperativity long reported with helix–coil transitions (e.g., Cantor and Schimmel, 1980). In the latter transitions, small changes in temperature (or solvent, etc.) can lead to sudden helical unwinding of polypeptides that otherwise prefer to be helical. Given the high helical content of spectrin, a comparison to such transitions would appear useful.

Forced unfolding often proceeds rapidly downhill beyond an initial transition or nucleation barrier (see Appendix 1) as illustrated most vividly perhaps in atomic scale simulations of spectrin (Paci and Karplus, 2000) as well as many other protein domains (Lu and Schulten, 1999). Such simulations show that relatively small sets of hydrogen bonds play critical roles in folding-unfolding mechanisms, as they do in helix–coil transitions (Cantor and Schimmel, 1980). Of course, with the α-, β-spectrin end constructs studied here, hydrogen bonds are central in stabilizing the helices. This stabilization would also apply to the supposed contiguous helix between serially adjacent repeats as documented in several spectrin family structures (Grum et al., 1999; Ylanne et al., 2001). Unfolding of one repeat might thus propagate by disrupting H-bonds and unfolding the connecting helix which extends into the serially adjacent repeat as one of the three helices. By this mechanism, unfolding of one such connecting helix would tend to open up the adjacent repeat's hydrophobic core and destabilize the repeat. Analogous to helix–coil transitions, such transitions are stochastic and expected to be sequence dependent, meaning some transitions are sharper, faster, and more cooperative than others.

Whether all spectrin repeats in αI- and βI-spectrin are connected by a contiguous helix that can propagate unfolding of tandem repeats is not clear. More flexibly linked repeats engineered for the studies of Lenne et al. (2000) were not reported to show tandem repeat unfolding events, which is consistent with the propagated unfolding mechanism proposed here. In addition, the initial results of Rief et el. (1999) on red cell spectrin suggest few tandem repeat events. Thus the cooperativity seen in the end domains here may prove more atypical than typical of spectrin.

Recent denaturation studies comparing one and two repeat spectrin constructs (chicken brain α-spectrin R16 and R17) in solution conclude that tandem repeats unfold at nearly the same temperature as single repeats and they do so only in concert as a single unit in an 'all or none' fashion, just as single repeat constructs do (MacDonald and Pozharski, 2001). Partially unfolded intermediate states are reported to be nonexistent in such studies. However, AFM-forced unfolding studies of spectrin by Lenne et al (2000) included experiments on the same domains and reported, as already cited, partially unfolded intermediates. Although Paci and Karplus (2000) have recognized that thermal denaturation pathways are generally distinct from forced unfolding pathways, the cooperative unfolding of repeats seen here under force nonetheless bears some resemblance to the cooperative unfolding in solution. One important distinction, however, is our finding that single repeat unfolding (i.e., partial unfolding of the construct) occurs with equal or greater frequency than tandem repeat unfolding by AFM. Even a small proclivity toward single repeat unfolding will tend to magnify single repeat unfolding at the expense of tandem repeat unfolding: for example, if just the second repeat is forced to unfold in a four repeat construct, then tandem unfolding of both repeats one-and-two and repeats two-and-three is no longer possible. Sequence differences among the various spectrin repeats studied might explain the different behaviors. Indeed, the solution unfolding studies of MacDonald and Pozharski (2001) show that addition of just a few amino acids can significantly change the unfolding free energy (by up to 30%). The different behavior might also reflect the fact that unfolding is forcibly done by AFM in milliseconds rather than the minutes or hours in the solution studies. In addition, the spectrin repeat unfolding lengths found here average only two thirds of the contour lengths and are also broadly distributed around this mean (see Fig. 6). This suggests that many repeats are not fully extended or even, perhaps, fully unfolded. In other words, many helix–coil transitions in forced unfolding of spectrin appear incomplete. This could prove physiologically important to the nucleation of refolding.

CONCLUSION

Cooperativity in either the association of proteins or the binding of ligands is both well-established and of obvious

physiological importance. Our results for spectrin indicate a similar level of complexity in the responses of protein domains to mechanical force. As is most clear from the two domain results, serially adjacent domains in a single spectrin chain appear to unfold cooperatively in tandem. Based on the various histograms and scatterplots, a relative frequency of tandem-to-single events is estimated to be between ~1:3 and 1:1, consistent with only a small difference in transition free energy. The mechanistic bases for this transition lies, we conclude, in the contiguous helix that interconnects repeats and cooperatively propagates unfolding. As graphically shown by recent simulations of mutant spectrins (Zhang et al., 2001), the subtle dependence of spectrin stability on specific residues is testament to the structural cooperativity that is intrinsic to individual spectrin domains. Equally important to the specific results found for spectrin, we suggest that full analyses of AFM unfolding results will tend to show that two proteins and loops are often forcibly extended in parallel. When this happens, domains in each chain will tend to unfold in close synchrony. This should also prove relevant to spectrin in the red cell which exists as an antiparallel heterodimer.

APPENDIX 1

Initial kinetic model of competing unfolding pathways

Both (Rief et al., 1999) and (Lenne et al., 2000) have shown that forced unfolding of spectrin exhibits a logarithmic (rather than proportional) dependence on loading or extension rate, as is commonly reported in these types of dynamic force experiments (Rief et al., 1997; Carl et al., 2001). With increasing rates of extension from 0.5 to 5 nm/ms for the $D = 4$ spectrin constructs here, we also find (data not shown) that unfolding forces increase by 20–30%. In addition, the bimodal distributions and scatterplots at the different rates show that the fraction ϕ of single repeat events is relatively constant at $\phi \sim 70 \pm 10\%$ (although Fig. 6 might suggest $\phi \sim$ 50%). Such results can be formally incorporated into an initial kinetic model of extensible unfolding of spectrin by amending a dynamic Monte Carlo integration method already applied to single repeat unfolding of spectrin (Rief et al., 1999) as well as other proteins (e.g., Rief et al., 1997; Carl et al., 2001). Two separate transition rates for single (^{s}) versus tandem (^{t}) repeats are coupled together:

$$k^s = N_f^s k_o^s \exp(-f x_u / k_B T) \tag{2a}$$

$$k^t = N_f^t k_o^t \exp[-f (x_u + \delta)/k_B T] \tag{2b}$$

where N_f denotes the number of folded domains at a given instant, k_o specifies the force-free rate of unfolding, and x_u (or $x_u + \delta$) indicates the unfolding distance from the folded state to the key transition state (Fig. 10 *A*). One expects that $k_o^t < k_o^s$ inasmuch as tandem repeats are likely to be more stable; in other words, in terms of transition state free energies with ΔG^* proportional to $-k_B T \log_n k_o$, one expects $\Delta G^{*t} > \Delta G^{*s}$. Equating the extra work for unfolding the tandem repeat at the same average force, $\langle f \rangle$, to the extra free energy that stabilizes the tandem repeat: $\Delta\Delta G = \langle f \rangle \delta$ which implies that $k_o^t = k_o^s \exp(\langle f \rangle \delta / k_B T)$. The four independent parameters of Eq. 2, a and b (k_o's, x_u's) are thus reduced to just three. Compared to simulations of single transitions, only one new parameter, δ, is thereby introduced, and this is adjusted numerically to match the experimental value of ϕ.

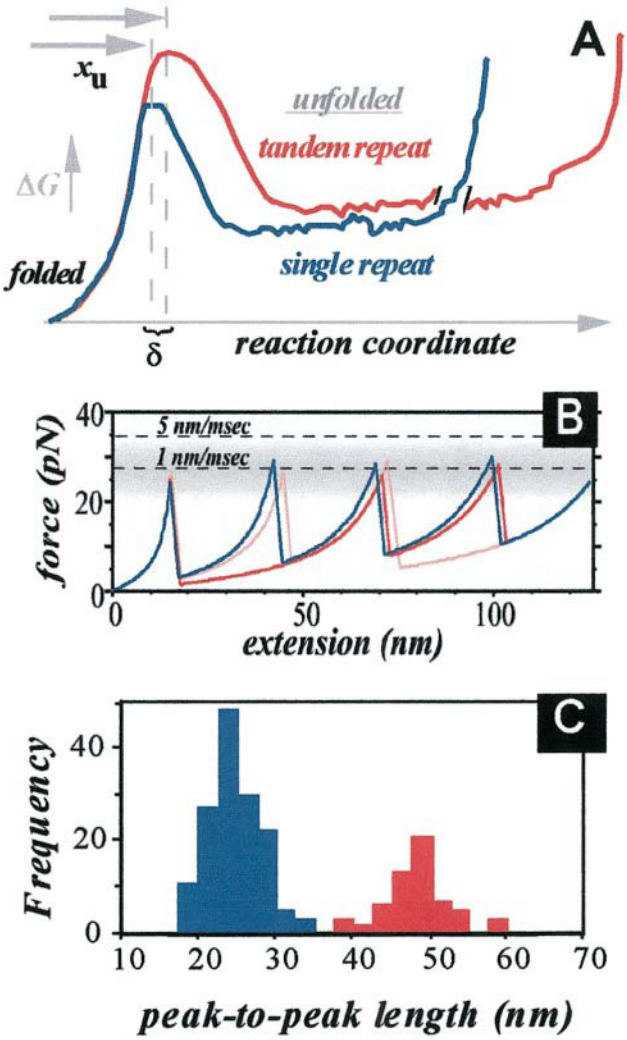

FIGURE 10 Simulated unfolding of single and tandem spectrin repeats. (*A*) Free energy profiles that underlie coupled Monte Carlo simulations described in the text by the coupled kinetics of Eq. 2, *a* and *b*. (*B*) Three extension curves for β_{1-4}-spectrin are shown. One spectrogram (in *blue*) shows four, single repeat unfolding events. The two other spectrograms (in *red*) show one tandem repeat unfolding event plus two, single repeat unfolding events. Appropriate contour lengths were taken from Table 1. The average force obtained at rates of extension of 1 or 5 nm/ms are indicated by the dashed lines; extension curves are for 1 nm/ms and the gray zone illustrates ±SD. (*C*) Histogram of the length between peaks in the simulated sawtooth patterns. The color code is used to distinguish single repeat (*blue*) from tandem repeat (*red*) events.

As indicated before, the full algorithm employing Eq. 2, *a* and *b* follows a Metropolis scheme that extends the chain at a chosen velocity (Rief et al., 1999, 1997; Carl et al., 2001) while attributing likelihood in proportion to transition rates (Eq. 2, *a* and *b*). The unfolding rates evolve with $f(x)$ and N; and for tandem repeat unfolding, we constrain unfolding to adjacent domains. Although parameters which adequately simulate experiment are generally not unique (Rief et al., 1999; Carl et al., 2001), representative values which match the measured unfolding force, its rate dependence, and the fraction of tandem unfolding events (Fig. 10, *B* and *C*) are in close agreement with prior fits of spectrin unfolding (Rief et al., 1999) with values of $x_u = 1.2$ nm and $k_o^s = 1/250\ s^{-1}$. The only new parameter needed for the fits is $\delta = 0.03\ x_u$ which clearly implies that the extra stability of a tandem

under force repeat is minimal versus a single repeat. Importantly, the simulated unfolding length distribution (Fig. 10 *C*) is bimodal with broad major and minor peaks centered at lengths which respectively correspond to single and tandem repeat unfolding events. Note also that these unfolding lengths are very close to those found in experiment at about two-thirds and four-thirds of the mean contour lengths adjusted from Table 1.

Note that in a prior review of this work, an anonymous reviewer with experience in titin unfolding remarked that ''Even in the case of the widely studied protein titin (8-Ig-domain constructs), only $<10\%$ of the data traces show 'clean' unfolding traces. For modular proteins with only four domains like in the present study, the success rate drops even more. An analysis of a four-domain titin construct would lead to the same broad force and peak distance distributions as in this study of spectrin. It is certainly not satisfying having to select data traces, but it seems the only way since interactions between tip surface and protein are complex and not understood in these experiments.'' However, the results here for spectrin—with typically 90–100% of the data analyzed—show reasonably well-defined and sensible averages compared to results for nonidentical but related spectrins by Rief et al. (1999) and Lenne et al. (2000). Admittedly, the widths of our experimental distributions are noise-limited compared to simulations (compare Figs. 6 and 10), but the distributions here still appear informative.

We thank George Liao, Carol Kwok, Judy Lin, and Lijoun Chen for invaluable assistance with the experiments as well as data analysis.

This work was supported by grants to D.W.S. and D.E.D. from the National Institutes of Health, the National Science Foundation, and the Muscular Dystrophy Association.

REFERENCES

Cantor, C. R., and P. R. Schimmel. 1980. Pt. III – The behavior of biological macromolecules. *In* Biophysical Chemistry. W.H. Freeman and Co., New York.

Carl, P., C. H. Kwok, G. Manderson, D. W. Speicher, and D. E. Discher. 2001. Forced unfolding modulated by disulfide bonds in the Ig domains of a cell adhesion molecule. *Proc. Natl. Acad. Sci. USA*. 98:1565–1570.

Coleman, T. R., D. J. Fishkind, M. S. Mooseker, and J. S. Morrow. 1989. Contributions of the beta-subunit to spectrin structure and function. *Cell Motil. Cytoskeleton*. 12:248–263.

Grum, V. L., D. Li, R. I. MacDonald, and A. Mondragon. 1999. Structures of Two Repeats of Spectrin Suggest Models of Flexibility. *Cell*. 98:523–535.

Kreis, T., and R. Vale. 1999. Guidebook to the Cytoskeletal and Motor Proteins. Oxford Univ. Press, New York.

Lee, J. C.-M., and D. E. Discher. 2001. Deformation-enhanced fluctuation in the red cell skeleton with theoretical relations to elasticity, connectivity, and spectrin unfolding. *Biophys. J*. 81:3178–3192.

Lenne, P.-F., A. J. Raae, S. M. Altmann, M. Saraste, and J. K. H. Horber. 2000. States and transitions during forced unfolding of a single spectrin repeat. *FEBS Lett*. 476:124–128.

Lu, H., and K. Schulten. 1999. Steered molecular dynamics simulations of force-induced protein domain unfolding. *Proteins*. 35:453–463.

MacDonald, R. I., and E. V. Pozharski. 2001. Free Energies of Urea and of Thermal Unfolding Show That Two Tandem Repeats of Spectrin Are Thermodynamically More Stable Than a Single Repeat. *Biochemistry*. 40:3974–3984.

Markle, D. R., E. A. Evans, and R. M. Hochmuth. 1983. Force relaxation and permanent deformation of erythrocyte membrane. *Biophys. J*. 42:91–98.

Marszalek, P. E., H. Li, and J. M. Fernandez. 2001. Fingerprinting polysaccharides with single-molecule atomic force microscopy. *Nat. Biotechnol*. 19:258–262.

Marszalek, P. E., H. Lu, H. Li, M. Carrion-Vazquez, A. F. Oberhauser, K. Schulten, and J. M. Fernandez. 1999. Mechanical unfolding intermediates in titin modules. *Nature*. 402:100–103.

Mohandas, N., and E. A. Evans. 1994. Mechanical properties of the red cell membrane in relation to molecular structure and genetic defects. *Annu. Rev. Biophys. Biomol. Struct*. 23:787–818.

Paci, E., and M. Karplus. 2000. Unfolding proteins by external forces and temperature: The importance of topology and energetics. *Proc. Natl. Acad. Sci. USA*. 97:6521–6526.

Rief, M., F. Gautel, F. Oesterhelt, J. M. Fernandez, and H. E. Gaub. 1997. Reversible unfolding of individual titin immunoglobulin domains by AFM. *Science*. 275:1295–1297.

Rief, M., J. Pascual, M. Saraste, and H. E. Gaub. 1999. Single Molecule Force Spectroscopy of Spectrin Repeats: Low unfolding forces in helix bundles. *J. Mol. Biol*. 286:553–561.

Shao, J.-Y., and R. M. Hochmuth. 1999. Mechanical Anchoring Strength of L-Selectin, 2 Integrins, and CD45 to Neutrophil Cytoskeleton and Membrane. *Biophys. J*. 77:587–596.

Ursitti, J. A., L. Kotula, T. M. DeSilva, P. J. Curtis, and D. W. Speicher. 1996. Mapping the human erythrocyte β-spectrin dimer initiation site using recombinant peptides and correlation of its phasing with the α-actinin dimer site. *J. Biol. Chem*. 271:6636–6644.

Waugh, R., and E. A. Evans. 1979. Thermoelasticity of red blood cell membrane. *Biophys. J*. 26:115–131.

Yang, G., C. Cecconi, W. Baase, I. Vetter, W. Breyer, J. Haack, B. Matthews, F. Dahlquist, and C. Bustamante. 2000. Solid-state synthesis and mechanical unfolding of polymers of T4 lysozyme. *Proc. Natl. Acad. Sci. USA*. 97:139–144.

Ylanne, J., K. Scheffzek, P. Young, and M. Saraste. 2001. Crystal structure of the alpha-actinin rod reveals an extensive torsional twist. *Structure*. 9:597–604.

Zhang, Z., A. W. Weed, P. G. Gallagher, and J. S. Morrow. 2001. Dynamic molecular modeling of pathogenic mutations in the spectrin self-association domain. *Blood*. 98:1645–1653.